14TH ITTC

SUBJECT : MANEUVERABILITY

AN AUTOMATIC MODEL TRACKING SYSTEM AT THE MANEUVERING TANK OF THE UNIVERSITY OF TOKYO

by T. Koyama, The University of Tokyo
S. Motora, Do.

1. Introduction

Since the maneuvering basin has been built in 1969, installation of new facilities had been promoted continuously.

In this year, the authors completed an automatic model tracking system for maneuvering tests which increased the ability of the X-Y carriage system to a large extent.

The configulation of this system is shown in the picture.

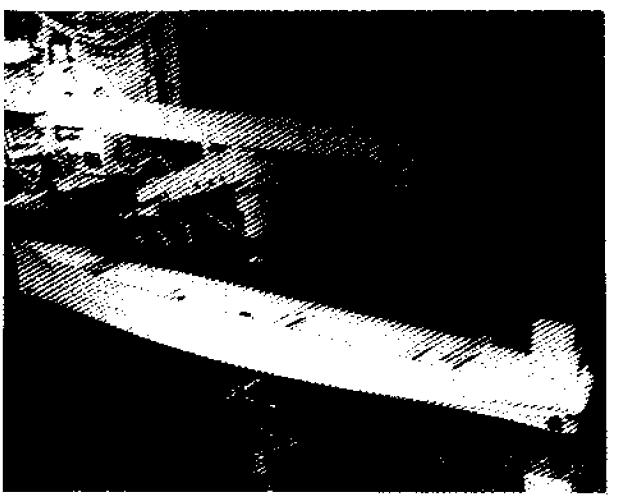

precision model tracking system
attached to the Y-carriage

The particular features of this system are as follows:

1. The trajectory of a model can be measured precisely.
2. The electric sources and the measurement signals

are transmitted by wires without any dynamic or static effects on models.
Consequently, even a free running test with a smaller size model can be made very easily.

Some improvements will be taken place for this system by computer which was installed on the X-carriage in October, 1974. The computer will be used for the digital control of X-Y carriages and data processing. Therefore, this report should be considered as an intermidiate one which only shows how the system works.

2. Dynamic characteristics of X-Y carriages and control sequence

The X-Y carriages at the maneuvering tank are constructed as a servo mechanisms so as to accept any kinds of control. Fig. 1 illustrates the general concepts of controls both for X and Y carriages.

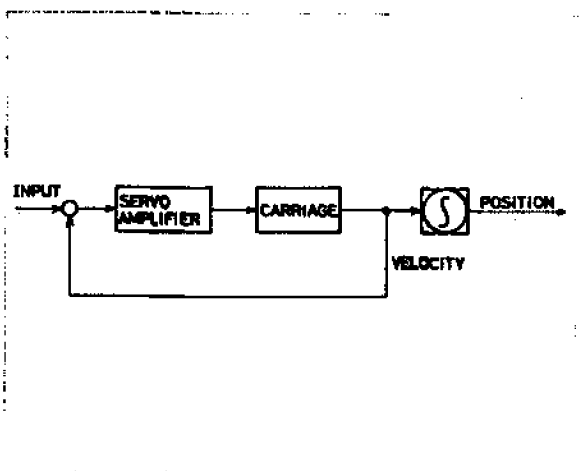

Fig. 1. Block diagram of the control for X and Y carriages

Any kinds of controls, for example, constant speed towing, oblique towing or manual model tracking, are made by applying an appropriate voltage signal to the input terminal of this system. The control system of carriages are made so flexible like this that only one thing we have to do is to measure the deviation of a model from the center of the sub-carriage and to put it into the input terminal in principle. However, it is not so simple in practice.

The frequency response characteristics of the X-Y carriages are shown in Fig. 2.

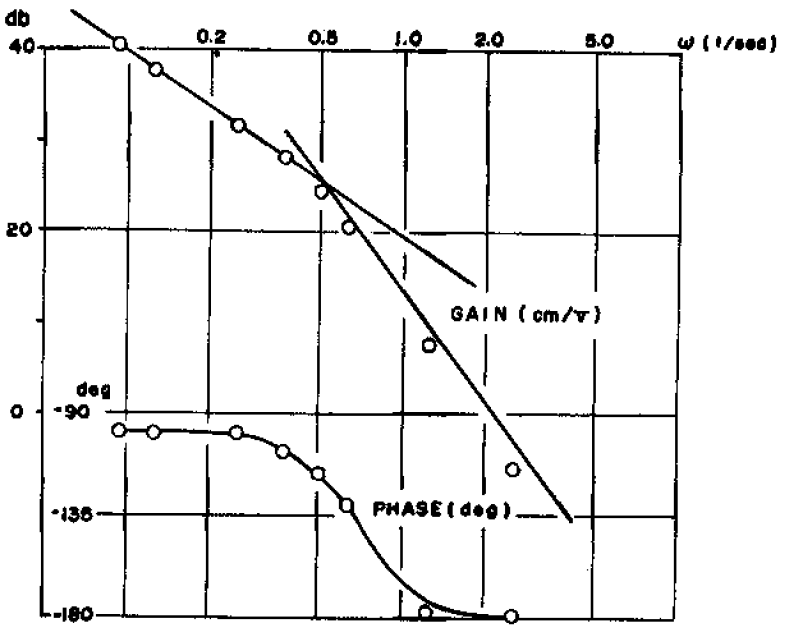

Fig. 2. Frequency response characteristics of X-Y carriages

The characteristics of X and Y carriages are not so different because of the feed back loop which is shown in Fig. 1. The time constant of carriages seems to be about 2 seconds which might be too large to track a model even for the maneuvering tests.

Analysis of these characteristics shows that the estimated tracking error will be at least ±40 cm if the automatic tracking is made directly by X-Y carriages. The large tracking error itself is not a problem in measuring the trajectory of a model. Because, if the tracking error can be measured precisely, the position of a model can be obtained by adding the carriage position and the tracking error. However, a rather large tracking error is very much inconvenient to connect a model and the sub-carriage by wires to transmit electric sources and measurement signals.

The two stages tracking system was employed to overcome this shortcoming. A precision tracking system was attached to the Y-carriage to interface the model and carriage position. This sequence is illustrated in Fig. 3.

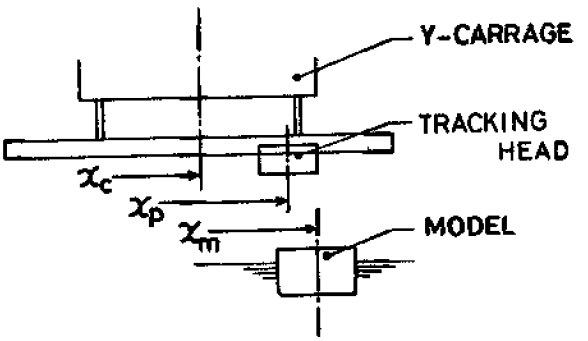

Fig. 3. 2-stages tracking system
x_m: position of a model
x_p: position of the tracking head
x_c: position of the carriage

A model (x_m) is tracked by the precision tracking head first, then the signal ($x_p - x_c$), which is the off-center component of the tracking system, is put into the carriage servo mechanism (Fig. 1) to form a feed back loop. Since the wires hang from the tracking head, and the head is kept right above the model, they have no effect on the model.

The span of the precision tracking system is one meter, so the allowable tolerance of carriage's tracking error is ±50 cm. This requirement is just enough for the maneuvering test using a 2.5 meters standard model.

3. Precision tracking system

The details of precision tracking system is shown in a picture at the beginning of this report. The span of this system is one meter for each X and Y directions, and the tracking head is driven by servo motors with sufficient power.

Optical sensors are provided to measure the signal of ($x_m - x_p$) in Fig. 3, which is the tracking error of the precision tracking system.

The light source is situated in a model, and the light from a model is received by optical sensing unit at the tracking head.

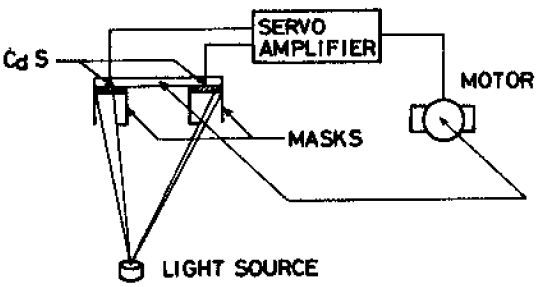

Fig. 4. Optical sensor for X and Y tracking

The optical sensing unit is composed of two sets of CdS (cadmium sulfite) elements and masks for X and Y direction. As illustrated in Fig. 4, masks make shadows on CdS element. If the output of these CdS elements are unbalanced, the servo motor drives the tracking head to balance them.

In order to connect the model and the tracking head with wires without any exciting forces on a model, the yawing tracking (ψ direction) must be made as well as X and Y directions.

For this purpose, an interesting sensor is attached to the tracking head.

The light source on a model is polarized by filter, and the two sets of CdS sensors receive this polarized light through polarizing filters which are mounted in rectangular directions each other (Fig. 5). Therefore, the output of CdS sensors are balanced only at the direction of 45 degrees to the polarized light field.

The tracking head has a short arm which is driven by this signal. This arm is used to hang wires to prevent any

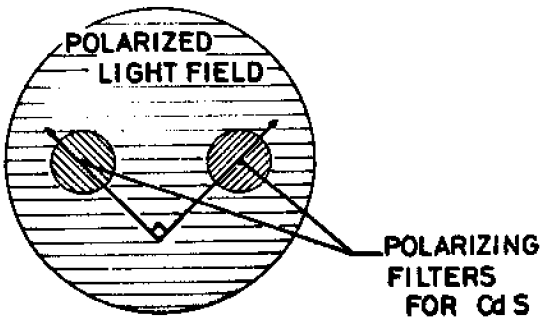

Fig. 5. ψ direction sensor with polarized light filters

forces acting on a model.

4. Some improvements in near future

At this moment, the automatic tracking system is working quite satisfactorily. However, following points are going to be improved by March, 1975.

(1) The position of X and Y carriages are measured by potentiometers. The accuracy of potentiometers is not sufficient to measure the span of 50 or 30 meters of X and Y carriages. The reversible counter will take the place of potentiometers to measure the position with the accuracy of 1 mm.

(2) In the case of a high speed model test, the span of the precision tracking is not sufficient for a normal PID control of carriages. Direct digital control by computer will improve this to a certain extent.

5. Acknowledgement

The authors acknowledge Professor Nakajima, Department of Mechanics, University of Tokyo, for his kindest suggestions in designing the precision tracking system and optical sensors.

14TH ITTC

SUBJECT : MANOEUVRABILITY

ANALOGUE ZIG-ZAG TEST ANALYSER

by K. Nomoto, University of Osaka
& K. Kose, University of Hiroshima.

1. Preface

There are various procedures of analysing the zig-zag test to obtain steering quality parameters of a ship; from the simplest method of the first-order (K and T) equation to the phase-plane analysis taking into account the higher order parameters and non-linearity.

In spite of the great developments in the PMM experiment plus digital simulation technique, this type of analysis will retain its important role, in this writer's view, for the time being. At least, in the analysis of actual ship trials, we have to solely rely upon it. Many model basins are, at the same time, still making a good deal of free-sailing model experiments as a rapid method of predicting the steering performance of a hull and/or rudder configurations.

The basic principle of this kind of analysis is to define a number of parameters of a mathematical model so that it fits with a detected ship motion and rudder movement as closely as possible. This may lead us to a simultaneous equations or some kind of the least square error method or iteration procedure.

One difficulty is that, the more the number of parameters to be defined, the more complicated the computation, and hence more error is introduced.

This note describes the application of the "visual iteration technique" for the analysis of zig-zag tests. To make the iteration on an analogue computer; adjust the parameters of the mathematical model built in the computer simply by turning a number of knobs whilst keeping an eye on the phase-plane trajectory displayed on a cathode-ray oscilloscope. Some of the results obtained are also indicated.

2. Mathematical Model and Basic Scheme of Analyser

The mathematical models employed are:

for a ship response,

$$\left.\begin{aligned} T_1 T_2 \dddot{\psi} + (T_1 + T_2)\ddot{\psi} + \dot{\psi} + \alpha\dot{\psi}^3 &= K\delta + KT_3\dot{\delta} \\ \delta &= \delta_m + \delta_r \end{aligned}\right\} \quad (1)$$

where ψ : yaw angle, δ_m : measured rudder angle and
δ_r : residual rudder angle (shift of the neutral position of the rudder)

and for a steering gear,

$$\left.\begin{aligned} T_E \dot{\delta}_m + \delta_m &= \delta_m^* && \text{when } \delta_m^* - \delta_m < \delta_c \\ T_E \dot{\delta}_m &= \delta_c && \delta_m^* - \delta_m \geq \delta_c \end{aligned}\right\} \quad (2)$$

where δ_m^* denotes the rudder angle command. Eq.(2) implies a first-order lag (exponential lag) with speed saturation, which is the common character of electro-hydraulic gears, δ_c being the saturation error signal.

It is possible to produce a certain sequence of time-varying electric voltage which simulates the rudder command record at the test. This signal is fed to an electric circuit whose response is described by Eqs.(1) and (2). We will then get a $\ddot{\psi} - \dot{\psi}$ phase-plane trajectory displayed on the oscilloscope, $\ddot{\psi}$ and $\dot{\psi}$ signals being fed out from the circuit. Repeating the rudder command sequence signal at a reasonably high frequency (the time scale in the simulation should have been adjusted so as to fit this operation), the trajectory remains bright on the display. Then we can adjust the parameters of Eq.(1) by turning the appropriate potentiometers so that the displayed trajectory coincide with the one obtained from the actual test. The latter trajectory is conveniently superimposed upon the former by means of a transparent paper or film.

In principle this visual iteration (trial and error procedure) could also be carried out in the time domain in place of the phase-plane, but the phase-plane is far preferable to the time history because the shape of the phase-plane trajectory reflects the characteristic parameters in a direct way and we can make use of this in the visual iteration.

The visual iteration on a phase-plane is applicable to any type of zig-zag manoeuvre, in fact to any type of steering test in principle. However, this procedure is most effective for the "limit cycle" zig-zag manoeuvres, which means the zig-zag with a fixed period and amplitude. For this type of zig-zag tests, we need not input any rudder command signal from outside. Instead, by adding a switching circuit which follows the rule of that zig-zag test (e.g. to put the rudder to the opposite side by a certain angle as soon as the heading deviation has reached a certain angle), the analogue circuit sets in the limit cycle by itself, simulating the limit cycle zig-zag motion of a ship.

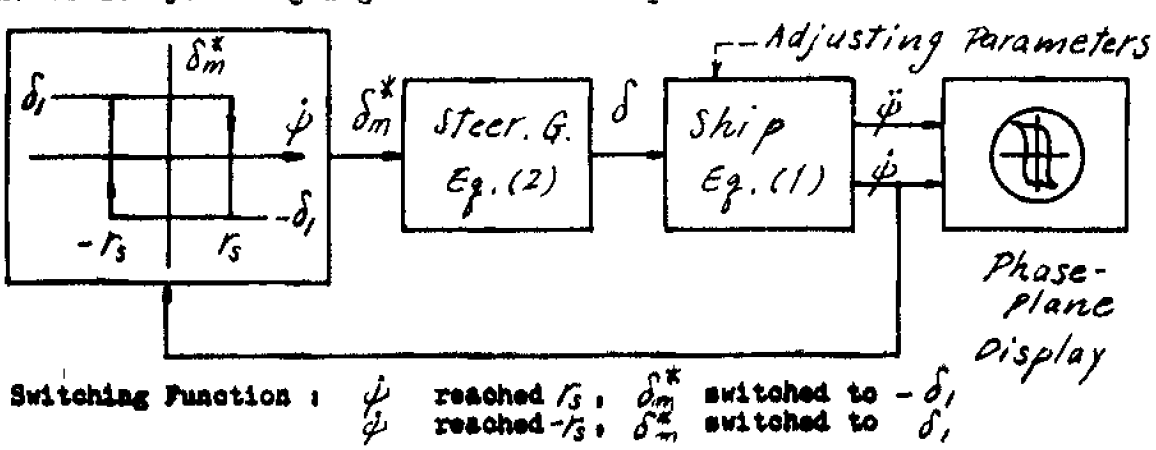

Fig.1. Yaw-rate Zig-zag Analyser --- Schematic Diagram.

Fig.1 shows a scheme of an analogue analyser for yaw-rate zig-zag tests, a typical limit cycle zig-zag manoeuvre.

A limit cycle zig-zag test is particularly suitable for the present approach, because:

(1) the phase-plane trajectory is a closed curve and thus the visual iteration is simple and accurate;
(2) the ship's phase-plane trajectory can be accurate by averaging over a number of periods. (cf. Section 4).

3. Actual Circuit and Procedure

A picture of the set-up is shown on Fig.2 and the block diagram of the circuit on Fig.3. All the operational amplifiers and the multipliers are of the module type on the market.

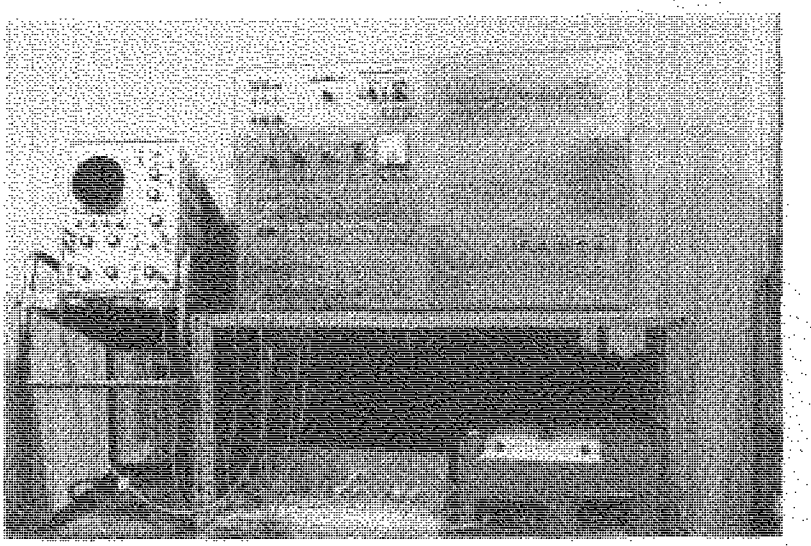

Fig.2. Zig-zag Test Analyser Set-up

The actual procedure of the visual iteration is:

(1) to adjust K by the slope of the trajectory at the $\dot{\psi}$ axis (i.e., so as to fit the displayed slope to the one obtained from an actual test), T_1 by the width of the trajectory along the $\dot{\psi}$ axis, and ψ_r by parallel shifting along the ψ axis ——— Step 1, Fig.4.
(2) to adjust α by curve fitting at the 1st and 3rd quarters——Step 2, and then make some correction to step 1 if needed,
(3) to adjust T_2 and T_3 by curve fitting at 2nd and 4th quarters and make final touch-up ——— Step 3.

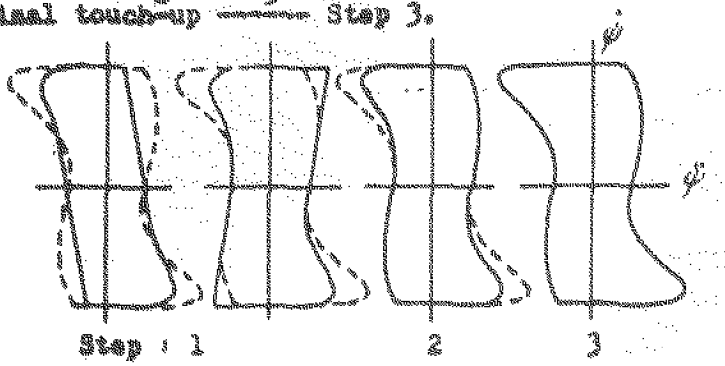

Fig.4. Procedure of Visual Iteration

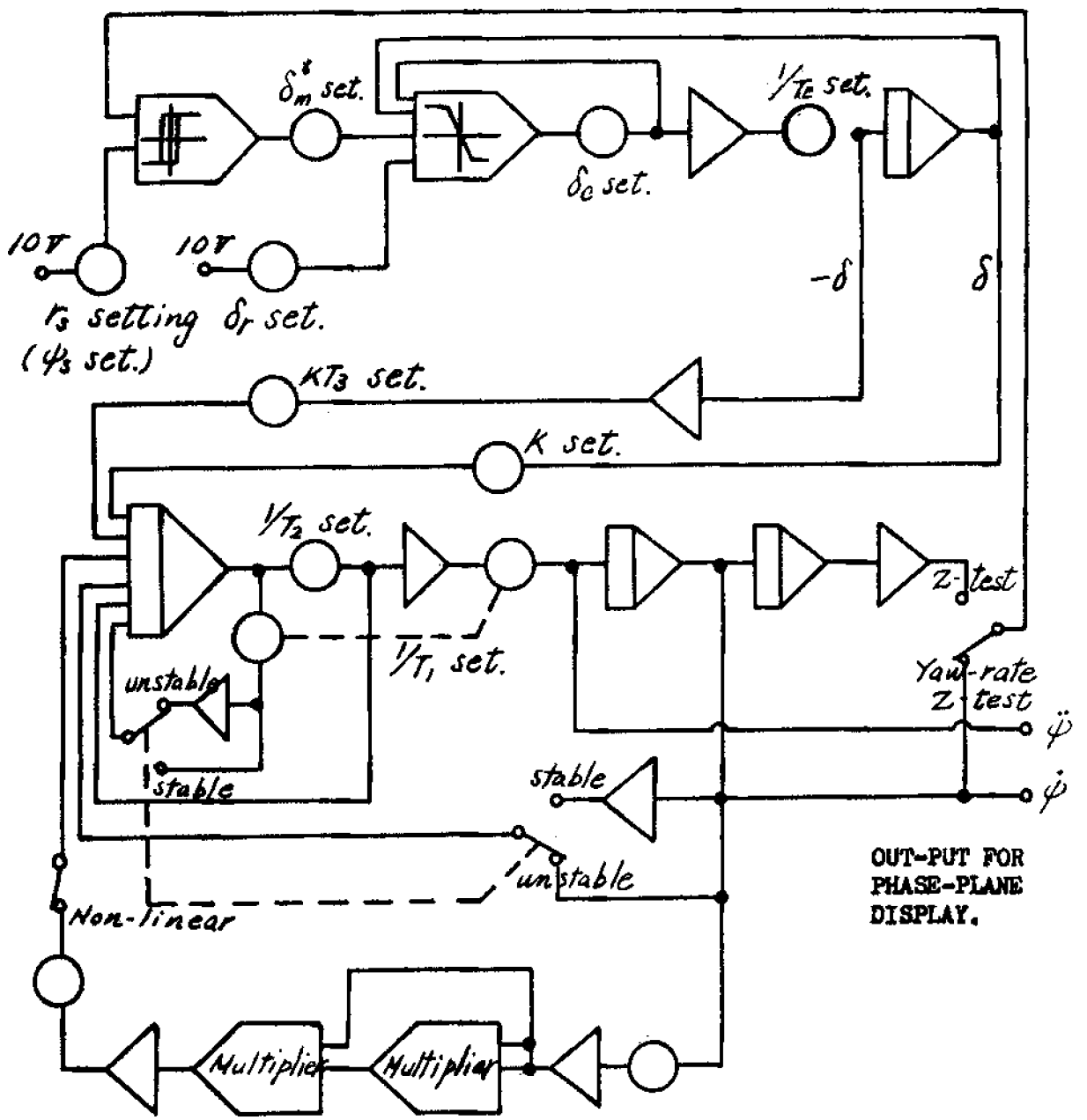

Basic Eqs. $T_1 T_2 \dddot{\psi} = K\delta + KT_3\dot{\delta} - (T_1 + T_2)\ddot{\psi} - \dot{\psi} - \alpha\dot{\psi}^3$

$T_E \dot{\delta}_m = \delta_m^* - \delta_m$ or $T_E \dot{\delta}_m = \delta_c$

Inverter Integrator Function Module

Potentiometer

Fig. 3. Circuit Diagram of Analogue Zig-zag Test Analyser.

4. Numerical Filtering of the Detected Ship Motion

The ship motion detected at a zig-zag trial is more or less distorted by miscelaneous sources and therefore it should be sent through a numerical filtering process prior to the analysis. The purpose of the process is to smoothen the measured yaw-rate signal and at the same time to give its differentiation with minimum possible noise.

Smoothing the yaw-rate signal is best performed with the filter weighting function:

$$w(t) = \frac{1}{2} \cdot \frac{\sin \omega_c t}{\pi t} \left(1 + \cos \pi \frac{t}{t_L} \right)$$

where ω_c denotes the cut-off frequency, and t_L the lag time, or the width of the "lag-window". The filtering process is described by the equation:

$$x(t) = \int_{t-t_L}^{t+t_L} x_r(\tau) \cdot w(t-\tau)\, d\tau \qquad (3)$$

where $x_r(t)$ denotes the given input with noise and $x(t)$ the filtered output. In this case x_r is the raw yaw-rate and x, the smoothened one.

The optimum cut-off frequency depends considerably upon the size and speed of a ship in question. As a temporary standard, ω_c should be

$10\pi(V/L)$ for the phase in which the rudder is moving and

$4\pi(V/L)$ for the phase in which the rudder is kept constant,

V being the ship speed and L the ship length. As for the lag time t_L, a sensible standard is apparently $t_L = 2\pi/\omega_c$. t_L is called upon to converge the integral of Eq.(3) in a reasonably short time.

Differentiating the yaw-rate signal gives the yaw-acceleration that will compose, together with the smoothened yaw-rate itself, the detected phase-plane trajectory for the analysis. This operation is performed with the filter weighting function:

$$w(t) = \frac{1}{2} \cdot \frac{\omega_c t \cos \omega_c t - \sin \omega_c t}{\pi t^2} \left(1 + \cos \pi \frac{t}{t_L} \right)$$

The input-output relation is described again by Eq.(3), but in this case x_r is the raw yaw-rate and x, the smoothened yaw-acceleration. The temporary standard for ω_c and t_L is the same as the above.

Here an emphasis should be laid upon the advantage of the zig-zag manoeuvres of an established limit cycle. For this kind of motion it is possible to get a nice phase-plane portrait by averaging over a number of cycles and with a relatively high cut-off frequency. From this point of view the yaw-rate zig-zag test as proposed at 13th ITTC is perhaps most suitable for this sort of analysis.

5. Examples

Table 1 indicates some results obtained. The car-ferry and the cutter have superior stability and very little non-linearity within the usual zig-zag motion. Most VLCC are more or less unstable on course and exhibit marked non-linearity.

In Fig.5 we compare the detected ship motion with the computed one using Eq.(1) and the parameters defined by the present approach. The agreement looks very good. Fig.6 illustrates some of the reverse spiral test results compared with the $r'-\delta$ characteristics that is composed from the parameters K and α obtained from zig-zag tests through the present analysis. The reverse spiral results of actual ships indicate some erroneous scatters but we can say that, on the whole, the agreement is reasonable.

Table 1. Steering Quality Parameters Obtained by Analogue Zig-zag Test Analyser.

	Actual Ships			Free Models	
	Car Ferry	Coast Guard Cutter	VLCC	VLCC	VLCC	VLCC
L	127 m	64.2 m	307 m	313 m	4.71 m	4.44 m
L/B	5.77	6.23	6.37	6.01	5.50	5.37
B/d	4.89	2.83	2.49	2.55	3.13	2.99
C_B	0.47	0.50	0.85	0.84	0.83	0.83
A_R/Ld	1/39	1/37	1/67	1/60	1/48	1/55
L/V	11.2 sec.	8.0 s	43.6 s	44 s	5.18 s	4.90 s
K	0.111 s^{-1}	0.113	-0.0345	-0.105	0.521	-0.385
T_1	23.8 s	14.5	-195	-654	32.1	-28.7
T_2	6.7 s	2.6	19	15	1.2	2.0
T_3	13 s	6.3	57	43	3.3	6.9
α	0.1 s^2deg^{-2}	0	-14.3	-23.7	0.05	-0.41
Remarks		Figs.5,6	Figs.5,6	Fig.6		

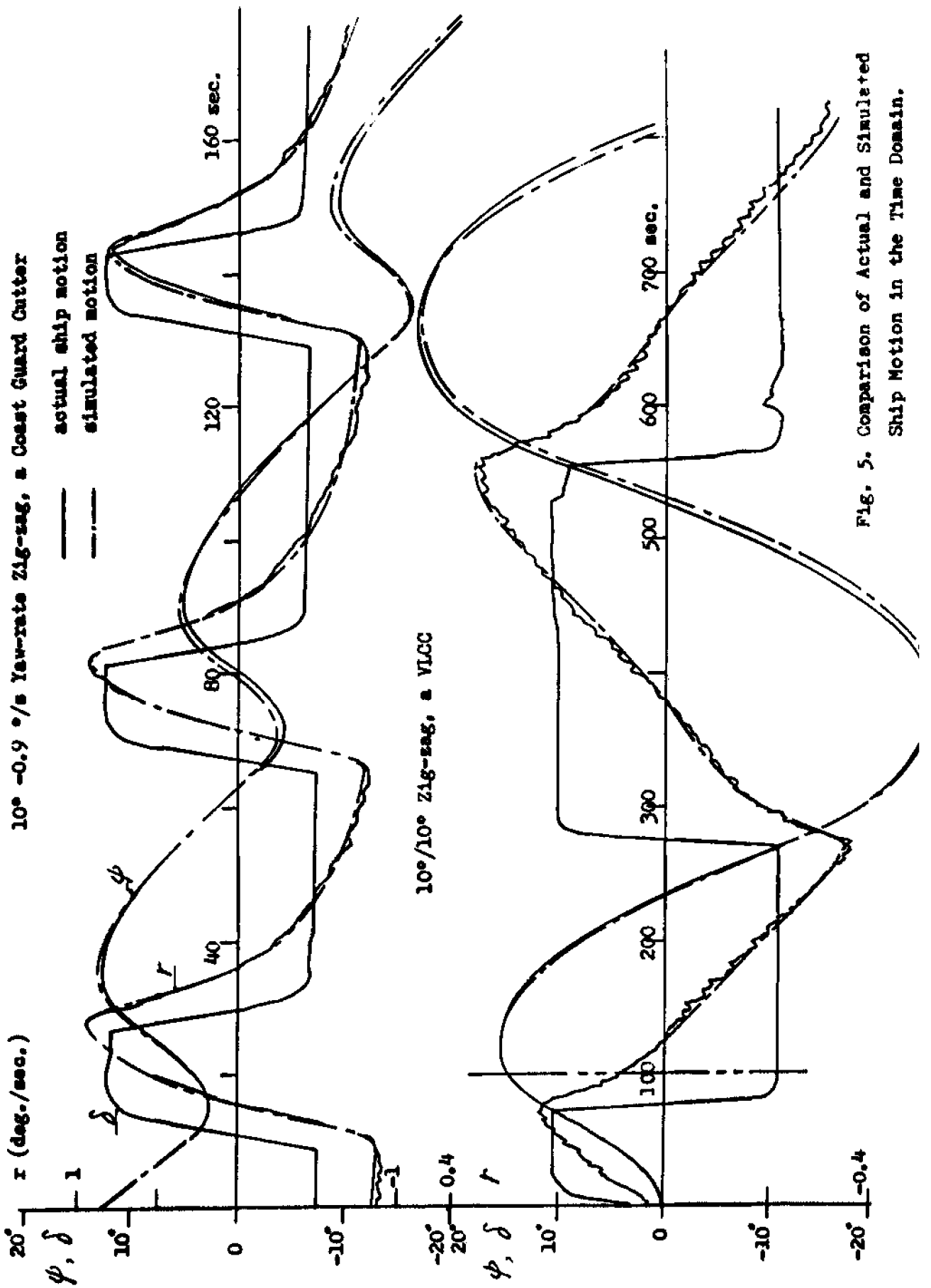

Fig. 5. Comparison of Actual and Simulated Ship Motion in the Time Domain.

o : Reverse spiral test plot

——·—— : r'- δ characteristic curve composed from K and α defined by analogue zig-zag analyser

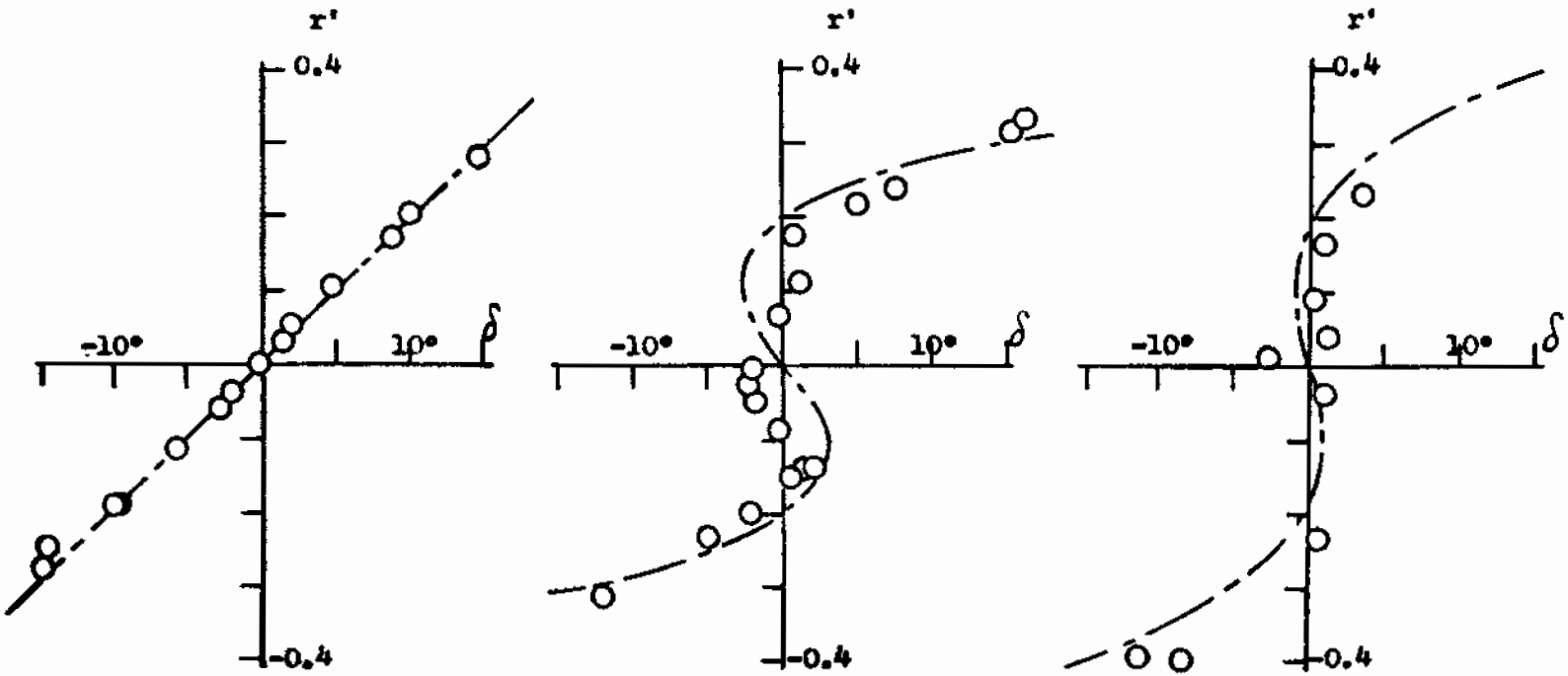

Coast Guard Cutter | 307 metre VLCC | 313 metre VLCC

Fig. 6. Simulated r'- δ Characteristics compared with Reverse Spiral Test Results